Structural insight into substrate specificity of medium-chain dehydrogenase reductase-type glucose dehydrogenase

Haruhiko Sakuraba[1]*, Kazunari Yoneda[2], Toshihisa Ohshima[3]

[1] Department of Applied Biological Science, Faculty of Agriculture, Kagawa University, 2393 Ikenobe, Miki-cho, Kita-gun, Kagawa761-0795, Japan
[2]Department of Bioscience, School of Agriculture, Tokai University, Kumamoto, Japan
[3]Department of Biomedical Engineering, Faculty of Engineering, Osaka Institute of Technology, 5-16-1 Omiya Asahi-ku, Osaka 535-8585, Japan

1 Introduction

Glucose dehydrogenase (GlcDH) catalyzes the oxidation of glucose to gluconate using NAD or NADP as a cofactor. To date, two types of GlcDH have been identified. The first type is classified as the short-chain dehydrogenase reductase (SDR) family. The SDR-type GlcDHs are found only in prokaryotes and insects. The second type of GlcDH occurs in archaea and belongs to the medium-chain dehydrogenase reductase (MDR) family. The archaeal MDR GlcDH is known to be the first enzyme in a non-phosphorylated variant of the Entner-Doudoroff pathway, which is utilized as the central sugar catabolic pathway in several thermoacidophilic archaea, most notably *Sulfolobus solfataricus*. GlcDH from *S. solfataricus* (ssGlcDH-1) shows activity toward a broad range of substrates, including D-glucose, D-galactose, D-xylose and L-arabinose [1]. Moreover, because metabolites of both D-glucose and D-galactose can utilized by the same enzymes in the pathway, it was proposed that the modified Entner-Doudoroff pathway in *S. solfataricus* is promiscuous for the metabolism of D-glucose and D-galactose. Recently, a second GlcDH (ssGlcDH-2) was identified in *S. solfataricus.* And because ssGlcDH-2 is absolutely specific for D-glucose, it is thought to be the major player in glucose catabolism via the modified Entner-Doudoroff pathway in *S. solfataricus*, whereas ssGlcDH-1 may have a dominant role in galactose degradation. To date, the crystal structures of MDR GlcDH from *T. acidophilum*, *S. solfataricus* (ssGlcDH-1) and *Haloferax mediterranei* have been reported. Extensive analysis of these structures has resolved the substrate binding sites and led to elucidation of the catalytic mechanism of these enzymes. However, there little is known about the mechanism underlying the differences in substrate-recognition among MDR GlcDHs, because the structure of a substrate-bound MDR GlcDH that shows narrow substrate specificity had not been determined.

In the present study, we succeeded in resolving the crystal structure of MDR GlcDH (tvGlcDH) from the thermoacidophilic archaeon *T. volcanium* in complex with D-glucose and nicotinic acid adenine dinucleotide phosphate (NAADP), an NADP analogue [2]. The amino-acid sequence of tvGlcDH showed 34% and 41% identity with those of ssGlcDH-1 and ssGlcDH-2, respectively, and the enzyme showed reactivity toward a strict range of substrates (D-glucose and D-galactose). A detailed structural analysis of tvGlcDH could shed light on the substrate-recognition mechanism of this enzyme, information that would provide further insight into the catalytic activity of MDR GlcDHs. We therefore compared the active-site architecture of tvGlcDH with that of ssGlcDH-1. We then evaluated the amino-acid residues that could be responsible for the difference of substrate specificity between tvGlcDH and ssGlcDH-1. This is the first description of the structure of a substrate-bound MDR GlcDH showing narrow substrate specificity.

2 Experiment

Diffraction data were collected (λ=1.0 Å) on the beamline AR-NW12 and AR-NE3A at the Photon Factory. The initial phases for the structure were determined by molecular replacement; the structure of chain A from ssGlcDH-1 (Protein Data Bank entry 2cd9) served as the search model.

3 Results and Discussion

In preliminary studies, we co-crystallized the tvGlcDH with NADP and determined the structure at a resolution of 2.6 Å. With this approach, however, we did not obtain a clear electron density for the NADP molecule, particularly for the nicotinamide ring moiety. This may reflect the relatively low resolution and partial occupancy of this portion. In ssGlcDH-1, NADP reportedly forms several specific interactions with residues in the nucleotide-binding site, one being a stacking interaction between one side of the nicotinamide ring and Phe277, while Phe279 stacks the other side of the nicotinamide ring. When we compared the structure of tvGlcDH with that of NADP-bound ssGlcDH-1 (2cda), we found that Phe279 in ssGlcDH-1 was replaced by Thr277 in tvGlcDH, though Phe277 was conserved as Phe275. We therefore constructed a T277F tvGlcDH mutant and then co-crystalized the mutant with NADP to solve the structure of NADP-bound T277F.

The maximum resolution of diffraction for NADP-bound T277F crystals was enhanced to 2.25 Å. As expected, the nicotinamide ring of NADP in T277F was tightly held at the active site via stacking interactions with Phe275 and Phe277. The electron density corresponding to the NADP bound within the nucleotide-binding site

was very clear, enabling us to place the ligand with reasonable accuracy.

Because tvGlcDH exhibits no detectable activity with nicotinic acid adenine dinucleotide phosphate (NAADP), crystals of NAADP-bound T277F mutant were prepared and then soaked in 1.8 M D-glucose. The model of the NAADP/D-glucose-bound T277F was refined at a resolution of 2.33 Å. The NAADP molecules in all four subunits were positioned/configured in a fashion nearly identical to the NADP molecule from the NADP-bound T277F structure. In the initial electron density map of NAADP/D-glucose-bound T277F, we observed an extra density within the active site cavity, and after construction and refinement of the peptide chain, a D-glucose molecule could be modeled into that density. Although detailed discussion of the structure of the C6-hydroxyl of D-glucose is difficult due to the poor electron density, the significant electron density at O1, O2, O3 and O4 enables us to deduce a reasonable positioning of the D-glucose molecule (Fig. 1).

In addition to the NADP/D-glucose-bound ssGlcDH-1 (T41A mutant) structure (2cdb), the crystal structure of ssGlcDH-1 (T41A mutant) in complex with NADP and D-xylose has been determined [1]. Comparison of this structure with that of NADP/D-glucose-bound ssGlcDH-1 revealed that the C2- and C3-hydroxyls of D-xylose are located at positions nearly identical to those of the corresponding hydroxyls of D-glucose in the glucose-bound structure. By contrast, the xylose ring appears to be pushed 0.9 Å away from the NADP nicotinamide ring at the pyranose oxygen (Fig. 2a). Consequently, the C1- and C4-hydroxyls of the xylose are also displaced 0.4 Å away from the position of the equivalent glucose atoms. Xylose, in contrast with glucose, has no C6-hydroxy group, and thus cannot form a hydrogen bond with His297* (asterisks indicate a residue in the neighboring subunit). The loss of this hydrogen bond is likely the main reason for the different positioning of the two sugars, as all other interactions between glucose and the enzyme are conserved in the xylose-bound structure. This suggests that the anchoring of the C2- and C3-hydroxyls of D-xylose at appropriate positions is important for its utilization as a substrate. By comparing the interactions around the C2- and C3-hydroxyls of the sugar between the substrate-bound ssGlcDH-1 and tvGlcDH structures, we found that the C3-hydroxyl of the sugar is tightly held at its position through 5 surrounding hydrogen-bonds in ssGlcDH-1 (Fig. 2a), whereas only 4 interactions were observed at the corresponding position in tvGlcDH (Fig. 2b). The number (3) of interactions between the sugar C2-hydroxyl and enzyme did not differ between the two enzymes. Given that xylose also cannot form the hydrogen bond with Glu296* in tvGlcDH, these observations suggest that the smaller number of interactions around at the C3-hydroxyl of the sugar weaken the affinity of tvGlcDH for D-xylose, making the binding insufficient for catalysis. Therefore, fewer interactions between the C3-hydroxyl group of the sugar and the enzyme are likely responsible for tvGlcDH's lack of reactivity towards D-xylose.
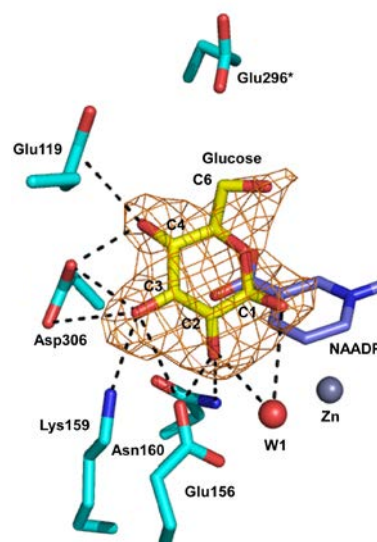
Fig. 1: D-glucose-binding site in tvGlcDH. W1 indicates a Zn-coordinated water molecule. The final σ_A-weighted F_o-F_c omit electron density map for D-glucose is shown at the 2.1 σ level.
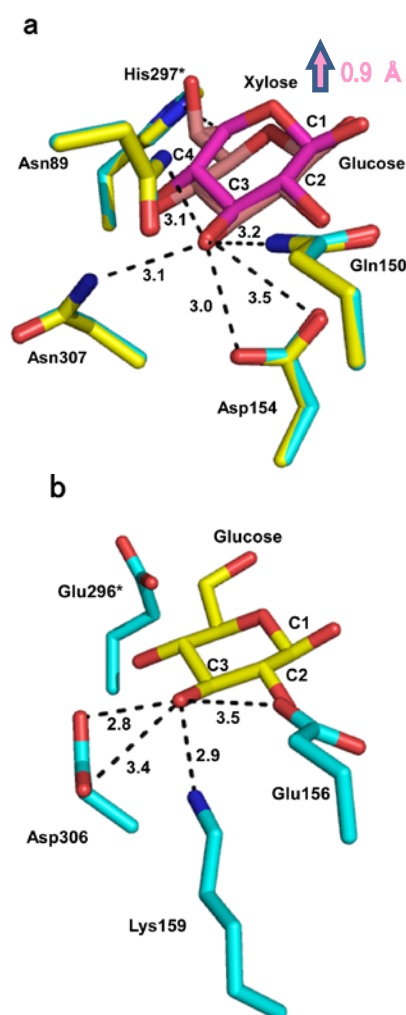
Fig. 2: Interactions around the C3-hydroxyls of the sugars. (a) The structure of D-glucose-bound ssGlcDH-1 (yellow) is superimposed on that of D-xylose-bound

ssGlcDH-1 (cyan).   (b) The structure of D-glucose-bound tvGlcDH. The interactions between C3-hydroxyls of the sugars and the surrounding residues are shown as dashed lines. Bonding lines were labeled with the corresponding distances (Å).

References
[1] C. C. Milburn *et al*., *J. Biol. Chem.* **281**, 14796 (2006).
[2] Y. Kanoh *et al*., *Acta Cryst.* **D70**, 1271 (2014).

* sakuraba@ag.kagawa-u.ac.jp